# Kinetic basis for insensitivity to tetrodotoxin and saxitoxin in sodium channels of canine heart and denervated rat skeletal muscle

**ARTICLE** *in* BIOCHEMISTRY · JANUARY 1988

Impact Factor: 3.02 · DOI: 10.1021/bi00398a003 · Source: PubMed



**6 AUTHORS**, INCLUDING:

Arippa Ravindran
U.S. Food and Drug Administration
**30** PUBLICATIONS **910** CITATIONS

SEE PROFILE

Edward G Moczydlowski
California Northstate University
**98** PUBLICATIONS **4,546** CITATIONS

SEE PROFILE

# Kinetic Basis for Insensitivity to Tetrodotoxin and Saxitoxin in Sodium Channels of Canine Heart and Denervated Rat Skeletal Muscle†

Xiaotao Guo,‡ Akira Uehara,§ Arippa Ravindran,∥ Shirley H. Bryant,‡ Sherwood Hall,⊥ and Edward Moczydlowski*,∥

*Department of Pharmacology and Cell Biophysics, University of Cincinnati College of Medicine, Cincinnati, Ohio 45267, Department of Physiology, Fukuoka University School of Medicine, Fukuoka, Japan, Department of Pharmacology, Yale University School of Medicine, New Haven, Connecticut 06510, and U.S. Food and Drug Administration, Washington, D.C. 20204*

*Received June 3, 1987; Revised Manuscript Received August 4, 1987*

ABSTRACT: The single-channel blocking kinetics of tetrodotoxin (TTX), saxitoxin (STX), and several STX derivatives were measured for various Na-channel subtypes incorporated into planar lipid bilayers in the presence of batrachotoxin. The subtypes studied include Na channels from rat skeletal muscle and rat brain, which have high affinity for TTX/STX, and Na channels from denervated rat skeletal muscle and canine heart, which have about 20–60-fold lower affinity for these toxins at 22 °C. The equilibrium dissociation constant of toxin binding is an exponential function of voltage ($e$-fold per 40 mV) in the range of −60 to +60 mV. This voltage dependence is similar for all channel subtypes and toxins, indicating that this property is a conserved feature of channel function for batrachotoxin-activated channels. The decrease in binding affinity for TTX and STX in low-affinity subtypes is due to a 3–9-fold decrease in the association rate constant and a 4–8-fold increase in the dissociation rate constant. For a series of STX derivatives, the association rate constant for toxin binding is approximately an exponential function of net toxin charge in membranes of neutral lipids, implying that there is a negative surface potential due to fixed negative charges in the vicinity of the toxin receptor. The magnitude of this surface potential (−35 to −43 mV at 0.2 M NaCl) is similar for both high- and low-affinity subtypes, suggesting that the lower association rate of toxin binding to toxin-insensitive subtypes is not due to decreased surface charge but rather to a slower protein conformational step. The increased rates of toxin dissociation from insensitive subtypes can be attributed to the loss of a few specific bonding interactions in the binding site such as loss of a hydrogen bond with the N-1 hydroxyl group of neosaxitoxin, which contributes about 1 kcal/mol of intrinsic binding energy.

The rapidly activating and inactivating inward current underlying the action potential of excitable cells is mediated by a class of membrane proteins called Na channels. Aside from their distinctive unitary conductance, ionic selectivity, and voltage dependence, Na channels are recognized by their sensitivity to a class of neurotoxins that includes heterocyclic guanidinium compounds such as tetrodotoxin (TTX)[1] and saxitoxin (STX) and also a group of 22 amino acid peptides called μ-conotoxins (Catterall, 1984; Cruz et al., 1985). Binding of these toxins to an extracellular site on the protein results in complete inhibition or block of the channel. The high affinity of these toxins for certain Na channels has been used to advantage in binding studies with tritiated toxins (Ritchie & Rogart, 1977) and in the purification of Na-channel proteins from electric organ (Miller et al., 1983), skeletal muscle (Kraner et al., 1985), and brain (Hartshorne & Catterall, 1984).

Electrophysiological and Na-flux measurements have demonstrated differences in the sensitivity of various tissues to these toxins (Catterall & Coppersmith, 1981; Frelin et al., 1984; Gonoi et al., 1985). For example, 1–10 nM TTX is sufficient to block Na currents in nerve and skeletal muscle, but 1–30 μM TTX is needed to block Na currents in mammalian heart (Baer et al., 1976; Brown et al., 1981; Cohen et al., 1981). Also, when rat muscle fibers are denervated by cutting the motor nerve, about 25–30% of the total Na current becomes insensitive to TTX ($IC_{50} \simeq 1$ μM) within a few days after denervation (Redfern & Thesleff, 1971; Pappone, 1980). This evidence, together with analogous binding studies using tritiated toxins (Rogart, 1986), can be used to distinguish a Na-channel subtype with low affinity for TTX that is present in heart and noninnervated skeletal muscle cells. Similarly, it has also been found that Na channels of adult mammalian skeletal muscle are much more sensitive to μ-conotoxin peptides than Na channels of brain and heart (Cruz et al., 1985; Ohizumi et al., 1986). Since the binding of STX, TTX, and μ-conotoxin is competitive and appears to involve a common overlapping binding site, pharmacology at this toxin receptor is a basis of discriminating three Na-channel subtypes present in mammals (Moczydlowski et al., 1986a): the m type of normal skeletal muscle has high affinity for TTX ($K_D \simeq 2$ nM) and μ-conotoxin ($K_D \simeq 30$ nM), the n type of neuronal tissues has high affinity for TTX ($K_D \simeq 1$ nM) but low affinity for μ-conotoxin ($K_D > 10$ μM), and the h type present in heart and denervated skeletal muscle has low affinity for both TTX

† This work was supported by NIH Grants AR38796 to E.M. and NS03178 to S.H.B. and by a grant to E.M. from the Searle Scholars Program/Chicago Community Trust. E.M. is supported by an Established Investigator award from the American Heart Association. X.G. is supported by a predoctoral fellowship from the Albert J. Ryan Foundation.

* Address correspondence to this author.
‡ University of Cincinnati College of Medicine.
§ Fukuoka University School of Medicine.
∥ Yale University School of Medicine.
⊥ U.S. Food and Drug Administration.

[1] Abbreviations: EDTA, ethylenediaminetetraacetic acid; Mops, 3-(*N*-morpholino)propanesulfonic acid; NEO, neosaxitoxin; STX, saxitoxin; dcSTX, decarbamoylsaxitoxin; TTX, tetrodotoxin.

0006-2960/87/0426-7546$01.50/0 

($K_D \simeq 1$ μM) and μ-conotoxin ($K_D > 10$ μM).

While the structural basis for these subtypes is unknown, suggestive evidence points to the analogy of isozymes where subtypes differ in primary sequence, being the product of homologous but distinct genes. This evidence derives from the isolation of two complete Na-channel cDNA clones that hybridize to rat brain mRNA and have only 87% sequence homology (Noda et al., 1986). Also, immunological studies have found instances where antibodies raised against purified Na channels from one tissue fail to recognize Na channels from other tissues or differentially stain separate regions of the same tissue (Fritz et al., 1983; Wollner & Catterall, 1985; Barchi, 1986).

The possible existence of such isochannels suggests that detailed comparison of functional properties of different subtypes could ultimately be used to correlate structural and functional alterations by use of such naturally occurring channel variants. In this paper we compare the toxin blocking kinetics of different Na-channel subtypes by TTX, STX, and a number of STX derivatives to arrive at a hypothesis for the molecular basis of differences in toxin sensitivity. Our methods involve the incorporation of single Na channels into artificial lipid bilayers in the presence of batrachotoxin, one of a class of lipophilic activating agents that stabilize the open state of Na channels at depolarized voltage and prevent voltage-dependent inactivation (Khodorov, 1985). With this technique, it is possible to observe the individual blocking events of guanidinium toxins binding to open channels (French et al., 1984; Moczydlowski et al., 1984a; Green et al., 1987a). By studying different channel subtypes after incorporation into the same lipid environment of the planar bilayer, we can examine functional differences between subtypes independently of membrane lipid composition. Using preparations of plasma membrane vesicles from canine heart and denervated skeletal muscle as a source of Na channels with low affinity for guanidinium toxins, we examine the kinetic basis for this low affinity. Preliminary descriptions of this work have appeared elsewhere (Guo et al., 1986; Moczydlowski et al., 1986b).

## Experimental Procedures

*Membrane Preparations and Toxins.* Native plasma membrane vesicles from various tissues were used for the incorporation of Na channels into planar bilayers. The final membrane pellet of each preparation was resuspended at 1–5 mg of protein/mL in 0.3 M sucrose buffer (10 mM Mops–NaOH, pH 7.4, 0.2 mM EDTA, 3 mM $NaN_3$) and stored in small aliquots at −80 °C.

Muscle membrane preparations were adapted from previous methods (Rosemblatt et al., 1981; Moczydlowski & Latorre, 1983) as follows. About 300 g of hind leg and back muscles was dissected from six male rats and collected in 0.3 M sucrose buffer at 0–4 °C. The muscle was divided into batches of 100 g and minced in a food processor. The minced tissue was combined with 300 mL of 0.3 M sucrose buffer and homogenized twice for 30 s at high speed in a blender. The homogenate was centrifuged for 10 min at 2500*g*. The supernatant was passed through cheesecloth, and solid KCl was added to a final concentration of 0.6 M. The suspension was stirred for 30 min, and crude microsomes were obtained as the pellet after centrifugation at 110000*g* for 45 min. The pellets were resuspended in 0.3 M sucrose buffer in a final volume of 50–100 mL. This suspension was centrifuged twice at 5000*g* for 10 min to remove a pellet containing mitochondria. About 8 mL of supernatant was layered over tubes containing 30 mL of 0.9 M sucrose buffer and centrifuged overnight at 85000*g*. Plasma membranes banding in the 0.3/0.9 M sucrose interface were collected, diluted by half with buffer, and pelleted at 110000*g* for 1 h.

A similar plasma membrane preparation was isolated from denervated rat muscle obtained as follows. A 1-cm piece of right sciatic nerve was surgically removed from 12 rats anesthetized with sodium pentobarbital. The incision was sutured and the animals were allowed to recover. At 5–7 days after surgery, only lower right leg muscle from each rat was dissected to provide about 30 g of tissue for the preparation. A scaled-down version of the preceding preparation was carried out after homogenization for 1 min in 5 volumes of 0.3 M sucrose buffer with a Polytron homogenizer at medium speed. The initial pellet was also rehomogenized and processed in the same manner to increase the yield of crude microsomes.

A preparation of sarcolemmal membranes from canine heart was developed from the methods of Van Alstyne et al. (1980) and the preceding skeletal muscle preparation. Ventricular muscle from one heart was minced and lightly homogenized in 5 volumes of 0.3 M sucrose buffer in a blender at the lowest speed for three bursts of 15 s separated by 15-s intervals. The suspension was centrifuged at 9000*g* for 20 min, and the supernatant was discarded. Four volumes of 0.3 M sucrose buffer was added to the pellets. This mixture was homogenized vigorously at high speed for 1 min and centrifuged as before, and the supernatant was filtered through cheesecloth and saved. The pellets were rehomogenized and centrifuged as in the preceding step, and the combined supernatants were pooled. Solid KCl was added to 0.6 M, and the suspension was stirred for 30 min and centrifuged at 110000*g* for 45 min. The pellets were resuspended in about 8 mL of 0.3 M sucrose buffer, and 2-mL portions of this suspension were layered over 20 mL of 0.7 M sucrose buffer and centrifuged at 80000*g* for 1 h. Plasma membranes banding at the 0.3/0.7 M sucrose interface were collected, diluted 3-fold with 0.3 M sucrose buffer, and pelleted at 110000*g* for 1 h. Membrane vesicles from rat brain were prepared as previously described (Moczydlowski et al., 1986a).

Derivatives of STX listed in Figure 7 were purified from cultures of *Protogonyaulax* and recrystallized as described previously (Hall, 1982). Decarbamoylsaxitoxin (dcSTX) was prepared by hydrolysis of saxitoxin as described (Ghazarossian et al., 1976). Toxin samples were used for analysis only when they exhibited single-exponential blocked time histograms characteristic of pure compounds.

*Planar Bilayers and Single-Channel Recording.* Planar bilayers were formed by the method of Mueller and Rudin (1969) by spreading a 25 mg/mL solution of phospholipids in decane over a 300-μm aperture in a polystyrene partition. Neutral lipid bilayers were formed from a mixture of 70% bovine brain phosphatidylethanolamine and 30% 1,2-diphytanoylphosphatidylcholine. In one set of experiments negatively charged membranes were formed from pure bovine brain phosphatidylserine. Lipids were purchased from Avanti Polar Lipids (Birmingham, AL) and shipped as chloroform solutions in sealed ampules. Bilayer formation was monitored by following the increase in membrane capacitance during membrane thinning. Ideal membranes for incorporation and recording of single Na channels had a capacitance in the range of 200–300 pF. All bilayer experiments were carried out at 21–24 °C with a solution of 200 mM NaCl, 0.1 mM EDTA, and 10 mM Mops–NaOH, pH 7.4, on both sides of the membrane. To incorporate batrachotoxin-activated Na channels, 0.2 μM batrachotoxin and 5–50 μg/mL membrane protein were added to one side of the bilayer with constant stirring. Channel incorporation usually occurred within 30

min after bilayer formation as monitored by an abrupt increase of about 1 pA of current at 50 mV. Only single-channel membranes were used for toxin blocking measurements.

Current was measured at constant voltage with a high-gain amplifier and a frequency compensation circuit similar to patch clamp design (Sigworth, 1983). Data were recorded on FM or VCR tape and analyzed after being filtered at 10–100 Hz (corner frequency, low-pass eight-pole Bessel filter). All voltages are referred by the physiological convention of extracellular ground as determined by use of the polarity of channel gating or toxin block to determine channel orientation. Where necessary, voltages were corrected for junction potentials by using the linear single-channel $I$–$V$ curves to measure the apparent reversal potential.

*Data Analysis.* Theory and methods for stochastic analysis of blocking events of single channels and applications to Na channels have been described previously (Colquhoun & Hawkes, 1983; Moczydlowski et al., 1984a; Green et al., 1987b). For toxins with slow kinetics (mean blocked time >2 s), the duration of blocking events was measured from chart records with the aid of a digitizing tablet (Houston Instruments, Austin, TX). For toxins with faster blocking kinetics, taped records were digitized at 100 Hz with a data acquisition system (Indec Systems, Sunnyvale, CA), and an event recognition program was used to tabulate blocking events by use of a discriminator set at 50% of the open channel current as an event criterion. The accuracy of measuring blocking events in this study was not limited by frequency response since toxins with the shortest dwell times exhibit mean blocked times greater than 0.3 s. Such events are cleanly resolved with 1-pA currents filtered at 100 Hz. A potential source of error is contamination of the blocking kinetics with brief channel gating events that exhibit closed times less than 0.2 s. This difficulty was overcome by selecting a cutoff time for the minimum length of blocking events as discussed previously (Moczydlowski et al., 1984a). This cutoff time was chosen in the range of 0.4–0.6 s for slow toxins and 0.1–0.2 s for fast toxins. In the latter case it was necessary to select channels with infrequent closings in the absence of blockers and to work at high toxin concentrations so that the frequency of blocking events is at least 50-fold greater than the frequency of gating events. the validity of this approach was demonstrated by single-exponential histograms and the independence of the measured mean blocked time on toxin concentration. Toxin rate constants were measured from samples of at least 50 events for a given channel and voltage. Rate constants were calculated from sample means or by fitting exponential dwell time histograms. Observed rate constants obtained from sample means were corrected for the closed cutoff time as described previously (Moczydlowski et al., 1984a). Rate constants in the range of −60 to +60 mV were fitted to exponential functions of voltage with a nonlinear least-squares minimization routine (DeCoursey et al., 1981).

## Results

*Identification of Single Toxin-Insensitive Na Channels.* Figure 1 shows current records from bilayers containing single batrachotoxin-modified Na channels from rat brain both in the absence of guanidinium toxins and in the presence of external TTX, STX, and neosaxitoxin (NEO) at concentrations that produce roughly 50% block. As previously reported (French et al., 1984; Hartshorne et al., 1985; Green et al., 1987a), batrachotoxin-modified Na channels from mammalian brain are open nearly all of the time at voltages more positive than −60 mV in the absence of guanidinium toxins, except for brief (<1 s) closing events that are due to a voltage-independent gating process. The addition of nanomolar concentrations of these toxins to the external side of the bilayer results in the appearance of discrete blocking events of many seconds in duration that correspond to the binding and unbinding of individual toxin molecules.

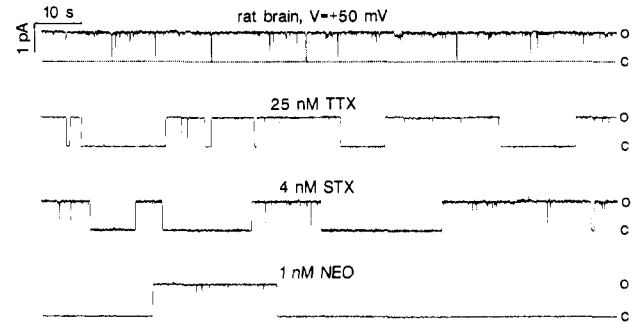


FIGURE 1: Toxin-sensitive Na channels from rat brain. Representative current records of single batrachotoxin-modified Na channels at +50 mV are shown in the absence of guanidinium toxins (top record) and in the presence of 25 nM TTX, 4 nM STX, or 1 nM NEO on the external side of the bilayer. The closed or blocked level is denoted by c and the open level by o. The solution on both sides of the bilayer was 10 mM Mops–NaOH, pH 7.4, 200 mM NaCl, and 0.1 mM EDTA. Rat brain Na channels were incorporated in the presence of 0.2 $\mu$M batrachotoxin.

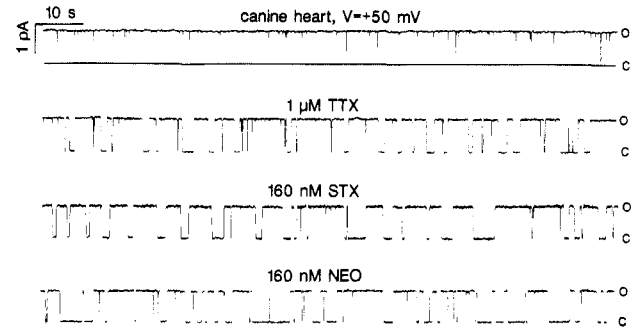


FIGURE 2: Toxin-insensitive Na channels from canine heart. Conditions were similar to those described in Figure 1 except that plasma membrane vesicles from heart ventricular muscle were used to incorporate Na channels. Note that higher concentrations of toxins are required for the same degree of block as for the brain channels in Figure 1. Note also the shorter lifetimes of blocked events in the presence of toxins as compared to Figure 1.

Records from similar experiments using canine heart preparations are shown in Figure 2 at the same gain and time scale as those of Figure 1. In the absence of guanidinium toxins, the behavior of the brain and heart channels is quite similar; however, about 40–200-fold higher toxin concentrations of these toxins are required for an equivalent blocking probability of the heart channel. Previous voltage-clamp experiments on single fibers of denervated rat skeletal muscle (Pappone, 1980) and patch-clamp experiments on cultured rat muscle cells (Weiss & Horn, 1986) identified two populations of Na channels with different sensitivity to TTX. The similar TTX insensitivity of Na channels in mammalian heart and a subpopulation of Na channels in noninnervated muscle suggests that these two channels may comprise a common pharmacological subtype. To investigate this question, we examined the properties of batrachotoxin-activated Na channels incorporated into artificial bilayers from plasma membranes of denervated rat muscle.

We found that two types of Na channels could be incorporated from this preparation as illustrated in Figure 3. Figure 3A shows current records of a single Na channel that exhibits roughly 50% block at 50 nM TTX, while Figure 3B shows a different channel that exhibits a similar blocking

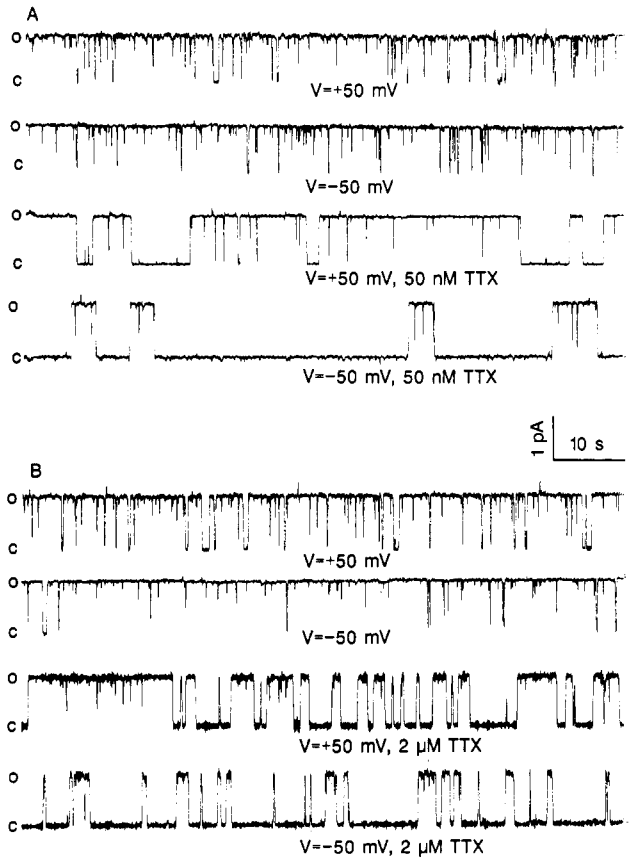


FIGURE 3: Two types of Na channels from denervated rat skeletal muscle: (A) records of a single toxin-sensitive Na channel; (B) records of a single toxin-insensitive Na channel. Conditions are similar to the experiments of Figures 1 and 2. Note the voltage dependence of blocking activity.

probability at 2 $\mu$M TTX. In this manner we are able to distinguish "TTX-sensitive" and "TTX-insensitive" subtypes from the same preparation that have respectively similar pharmacological properties to the TTX-sensitive channel from brain in Figure 1 and the TTX-insensitive channel from heart in Figure 2. While we observe the incorporation of exclusively TTX-sensitive Na channels from rat brain or normal rat muscle and exclusively TTX-insensitive Na channels from canine heart, the denervated muscle membrane preparation gives a mixture of these two types of Na channels.

Figure 3 shows rare records from bilayers containing single channels of either type, but most experiments with the denervated muscle preparation result in the incorporation of more than one channel, and a given bilayer often contains both types of channels oriented in either direction. For such multichannel membranes it is possible to count the number of each channel type. In practice this is done by measuring the current in the absence of TTX, dividing by the unitary current to obtain the total number of channels, and then counting the number of channels that remain after the consecutive addition of 1 $\mu$M TTX to both sides of the bilayer. Under these conditions at −50 mV, the TTX-sensitive channels are blocked about 99% of the time and appear as very brief opening transitions, while the TTX-insensitive channels are only blocked 70% of the time and exhibit well-resolved opening transitions as in Figure 3B. Careful records of the numbers of each channel type were taken for 54 different bilayers. In these experiments we counted a total of 110 Na channels of which 23 were TTX-insensitive and 87 were TTX-sensitive. Our observed proportion of 21% TTX-insensitive channels is similar to the fraction of the TTX-insensitive macroscopic current reported in voltage-clamp experiments with denervated rat muscle fibers (Pappone, 1980). This suggests that the incorporation probability is approximately equal for both types of channels.

Figure 3 also illustrates the voltage dependence of the TTX block of BTX-modified channels in a comparison of records taken from the same bilayer at +50 and −50 mV. This phenomenon was first described by Krueger et al. (1983) for batrachotoxin-modified rat brain Na channels and was later confirmed in other preparations (Green et al., 1987b; Moczydlowski et al., 1984a). These previous studies showed that the probability of toxin block is enhanced with increasing negative membrane potential and is the result of an increase in the mean blocked dwell time and a decrease in the mean unblocked dwell time. Figure 3B shows that a similar voltage-dependent block is observed for the TTX-insensitive subtype of denervated rat muscle.

The data of Figures 1–3 also show that the size of the unitary currents of BTX-modified channels is similar for various subtypes incorporated into bilayers of the same lipid composition. However, precise measurements of conductance from single-channel current–voltage data at 0.2 M NaCl (data not shown) reveal that there is a significant difference ($P < 0.01$) between TTX-sensitive channels from normal (20.0 ± 1.1 pS) or denervated muscle (19.7 ± 0.5 pS) and TTX-insensitive channels from heart (22.1 ± 0.8 pS) or denervated muscle (22.5 ± 0.5 pS). While our results indicate that TTX-insensitive channels have a 10% larger conductance than TTX-sensitive channels, Weiss and Horn (1986) found an opposite result with 22% larger conductance for TTX-sensitive channels in cell membrane patches. These contrasting results could be due to a difference between normal and BTX-modified channels or to the different ionic conditions of these experiments. In any case, the conductance difference between channel subtypes suggests that other functional properties besides toxin binding may also vary among subtypes. Indeed, we have recently observed that the heart Na channel is much more sensitive to block by certain divalent cations such as $Zn^{2+}$ (Moczydlowski, unpublished results) as also found in $^{22}Na$-flux studies by Frelin et al. (1986).

*Analysis of TTX Blocking Kinetics.* For Na channels with high affinity for TTX/STX, such as those from rat brain (French et al., 1984) and skeletal muscle (Moczydlowski et al., 1984a), the discrete blocking behavior of batrachotoxin-modified channels is predicted by reversible binding of a toxin, T, to a single site according to

$$O + T \underset{k_d}{\overset{k_a}{\rightleftharpoons}} O{\cdot}T \qquad (1)$$

where O and O·T refer to the open or unblocked channel and the toxin-blocked channel, respectively, and $k_a$ and $k_d$ are the respective association and dissociation rate constants for toxin binding. For a single channel exhibiting this behavior, the blocked events correspond to the random times that a toxin molecule resides on the blocked channel before it dissociates, and the unblocked events correspond to the random waiting time of an unoccupied channel before it binds another toxin molecule. The populations of blocked and unblocked events are described by an exponential distribution according to

$$P(\tau_i > t) = \exp(-kt) \qquad (2)$$

where $P(\tau_i > t)$ is the cumulative probability of events lasting longer than time, $t$, and $k$ is the observed rate constant. Equations 3 and 4 give the relationships between the observed

$$k_b = \bar{\tau}_b^{-1} = k_d \qquad (3)$$

$$k_u = \bar{\tau}_u^{-1} = [T]k_a \qquad (4)$$

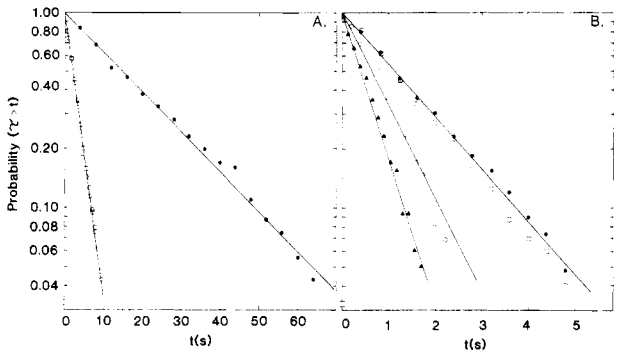


FIGURE 4: Cumulative probability histograms of blocked and unblocked events in the presence of TTX at −50 mV. (A) Blocked events of TTX-sensitive channels from denervated skeletal muscle [(●) 0.1 μM TTX, $\tau$ = 21.3 s, $n$ = 161] and TTX-insensitive channels from denervated skeletal muscle [(○) 1 μM TTX, $\tau$ = 3.47 s, $n$ = 305] or canine heart [(□) 1 μM TTX, $\tau$ = 3.64 s, $n$ = 382]. (B) Unblocked events of TTX-insensitive channels from canine heart [(●) 1 μM TTX, $\tau$ = 1.62 s, $n$ = 379; (○) 2 μM TTX, $\tau$ = 0.92 s, $n$ = 202; (▲) 4 μM TTX, $\tau$ = 0.58 s, $n$ = 180] and denervated skeletal muscle [(□) 1 μM TTX, $\tau$ = 1.51 s, $n$ = 301]. The individual event histograms contain data pooled from one to three single channel membranes.

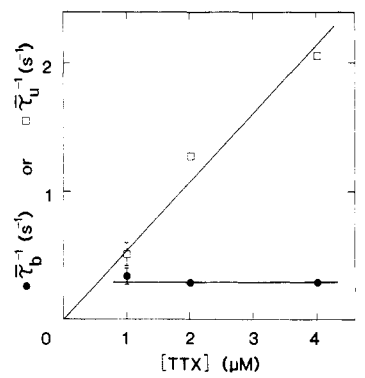


FIGURE 5: Dependence of reciprocal mean blocked ($\bar{\tau}_b$) and mean unblocked ($\bar{\tau}_u$) times on TTX concentration for TTX-insensitive Na channels from canine heart. Mean dwell times of 130–380 events were measured at −50 mV and at 1, 2, or 4 μM TTX. The observed means were corrected for a cutoff limit for short blocking events of 0.6 s as described under Experimental Procedures. The solid line fits correspond to an association rate constant of 5.4 × 10$^5$ s$^{-1}$ M$^{-1}$ (□) and a dissociation rate constant of 0.30 s$^{-1}$ (●), giving a $K_D$ of 0.56 μM at this voltage.

rate constants of the blocked ($k_b$) and unblocked ($k_u$) populations, the mean dwell time of the populations, $\bar{\tau}_b$ and $\bar{\tau}_u$, and the actual binding rate constants of eq 1. Thus the mean blocked dwell time is expected to be independent of toxin concentration, while the mean unblocked dwell time is inversely proportional to the toxin concentration. To investigate the kinetic basis of TTX insensitivity, we applied this kinetic analysis to Na channels from heart and denervated muscle.

Figure 4 shows cumulative probability histograms of blocked and unblocked events from single-channel records taken at −50 mV of several different Na-channel subtypes in the presence of TTX plotted according to eq 2. Both the blocked and unblocked histograms are well described by single exponentials as predicted by eq 1 and 2. Figure 4A shows that the TTX-sensitive channel from denervated rat skeletal muscle has a longer mean blocked time ($\bar{\tau}_b$ = 21.3 s) than the TTX-insensitive channel from denervated rat muscle ($\bar{\tau}_b$ = 3.5 s) or canine heart ($\bar{\tau}_b$ = 3.6 s). These results verify that the reduction in toxin affinity is due to a faster dissociation rate constant in the toxin-insensitive subtypes and also reveal a close similarity of the off rates for TTX-insensitive channels from two different species and tissues. Figure 4B shows that the mean dwell time of unblocked events shortens with increasing TTX concentration for the subtype from canine heart as expected from eq 4. This figure also indicates close similarity of the unblocked dwell time data for the canine heart Na channel and the TTX-insensitive channel from denervated rat muscle at 1 μM TTX. The dependence of the reciprocal mean blocked and unblocked dwell times on TTX concentration for the canine heart channel is shown in Figure 5. In agreement with eq 3 and 4, the reciprocal of the mean unblocked time is linearly related to TTX concentration while the mean blocked time is independent of toxin concentration. These data can be used to calculate an association rate constant of 5.4 × 10$^5$ s$^{-1}$ M$^{-1}$, a dissociation rate constant of 0.30 s$^{-1}$, and an equilibrium dissociation constant of 560 nM at −50 mV.

Similar methods were used to measure and compare the voltage dependence of TTX blocking of single channels from canine heart, normal rat muscle, and denervated rat muscle. We found that the derived dissociation and association rate constants for toxin blocking of the TTX-insensitive subtypes could be fit to exponential functions of voltage in the range of −60 to +60 mV as described previously for various TTX-sensitive subtypes (French et al., 1984; Moczydlowski et al., 1984a; Green et al., 1987b). These relations can be expressed as

$$k_d(V) = k_d(0)\ \exp(z_d'FV/RT) \quad (5)$$

$$k_a(V) = k_a(0)\ \exp(-z_a'FV/RT) \quad (6)$$

$$K_D(V) = K_D(0)\ \exp(z'FV/RT) \quad (7)$$

where $k_d(0)$ and $k_a(0)$ are the dissociation and association rate constants at 0 mV, $K_D(V)$ is the equilibrium dissociation constant equal to the ratio of $k_d(V)/k_a(V)$ and the parameters $z_d'$, $z_a'$, and $z'$ are effective valences that describe the voltage dependence of these processes (Woodhull, 1973). Figure 6 shows semilogarithmic plots of rate constants vs voltage for TTX blocking of different subtypes. The results show that the voltage dependence of TTX blocking as visualized in the slopes of the fitted lines in Figure 6 is not significantly different for the TTX-sensitive and TTX-insensitive subtypes. Thus, the difference in binding affinity is reflected exclusively in the zero-voltage rate constants as indicated by the vertical displacement of the data for TTX-sensitive and -insensitive channels. Figure 6 also shows that the kinetics of TTX blocking for TTX-insensitive channels from canine heart and denervated rat muscle are practically indistinguishable in planar bilayers. Also, the kinetics of TTX-sensitive channels from normal or denervated rat muscle are not significantly different. The experiment of Figure 6 allows us to conclude that the low affinity for TTX in the insensitive channel of heart and denervated muscle is the result of the combined effects of a 4-fold faster dissociation rate and a 7-fold slower association rate, resulting in a 30-fold difference in the equilibrium binding constant.

*Molecular Basis of Low Affinity Investigated with Saxitoxin Derivatives.* Figure 7 shows the structure of STX and a number of naturally occurring STX derivatives that have been previously used to probe the toxin binding site of Na channels with high affinity for TTX and STX (Kao & Walker, 1982; Strichartz, 1984; Kao, 1986; Moczydlowski et al., 1984b). We used several of these toxins to compare the single-channel blocking kinetics of both high- and low-affinity subtypes as described for TTX in the preceding section. Table I is a summary of kinetic parameters for various toxins that includes updated data from previously published experiments with normal rat muscle (Moczydlowski et al., 1984b, 1986c) and additional subtypes investigated in the present study.

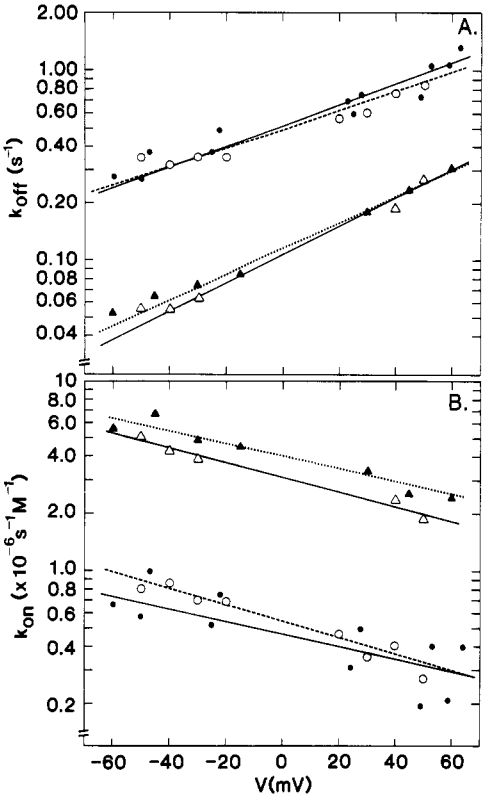


FIGURE 6: Voltage dependence of TTX binding rate and equilibrium constants for different subtypes of batrachotoxin-modified Na channels: (A) dissociation rate constant; (B) association rate constant. (▲) TTX-sensitive channel from normal rat muscle; (△) TTX-sensitive channel from denervated rat skeletal muscle; (○) TTX-insensitive channel from denervated rat skeletal muscle; (●) TTX-insensitive channel from canine heart. Data for each channel type were pooled from five to six single channel membranes with 100–600 events for each point. Solid lines through the data were drawn according to nonlinear least-squares fits to exponential functions of voltage with best-fit parameters given in Table I.

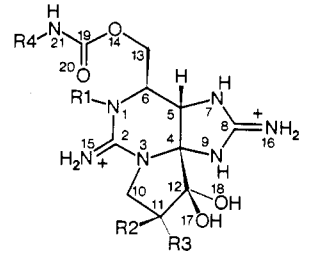

| | R1 | R2 | R3 | R4 |
|---|---|---|---|---|
| STX | H | H | H | H |
| B1 | H | H | H | $SO_3^-$ |
| GTX2 | H | H | $OSO_3^-$ | H |
| C1 | H | H | $OSO_3^-$ | $SO_3^-$ |
| GTX3 | H | $OSO_3^-$ | H | H |
| C2 | H | $OSO_3^-$ | H | $SO_3^-$ |
| NEO | OH | H | H | H |
| B2 | OH | H | H | $SO_3^-$ |
| GTX1 | OH | H | $OSO_3^-$ | H |
| C3 | OH | H | $OSO_3^-$ | $SO_3^-$ |

FIGURE 7: Structures of naturally occurring saxitoxin derivatives used in this study.

The results show that the effective valence, $z'$, measured for the voltage dependence of the equilibrium binding constant, does not vary significantly for different toxins or for different channel subtypes. The mean value of $z'$ is 0.63 ± 0.07 (SD) for all 26 measurements. The lack of dependence of this parameter on the net charge or structure of the various derivatives in Figure 7 has previously been used to conclude that the voltage dependence of binding does not arise as a result of direct toxin entry into the transmembrane electric field (Moczydlowski et al., 1984b). These and similar results have led to the consensus that the toxin binding site is situated outside of the membrane on an extracellular portion of the protein (Krueger et al., 1986; Green et al., 1987b).

The voltage dependence of binding has been proposed to arise from an allosteric interaction of the toxin binding site with voltage-sensing regions of the protein that do lie within the membrane. This model has been formalized as a voltage-dependent equilibrium of high- and low-affinity conformations linked with voltage-independent toxin binding reactions (Moczydlowski et al., 1984b) or as a voltage-dependent conformational change that closes the channel subsequent to toxin binding (Green et al., 1987b). The data of Table I imply that the structural features responsible for the voltage dependence of toxin binding to batrachotoxin-modified channels are highly conserved among various Na-channel subtypes. Table I also shows that in many cases the $z_a'$ and $z_d'$ terms are of roughly equal magnitude for the association and dissociation reactions, implying a fairly symmetrical energy barrier. However in some cases most of the voltage dependence is found in either the forward or reverse reaction. This peculiarity has also been noted for TTX and STX blocking of the canine brain Na channel by Green et al. (1987b). The origin of these variations remains obscure since we do not find any consistent correlation of these differences with toxin structure.

Comparison of the zero-voltage rate constants of STX and its derivatives among various Na-channel subtypes (Table I) reinforces our basic findings with TTX in the preceding section. In cases where a particular toxin has lower affinity for an h-type Na channel, this is the combined result of both a slower association rate constant and a faster dissociation rate constant.

Previous work on Na channels with high affinity for TTX/STX has established that electrostatic interactions play a major role in determining the apparent binding affinity of these toxins (Henderson et al., 1974; Hille et al., 1975; Grissmer, 1984; Strichartz et al., 1986). Most recently Green et al. (1987b) have proposed a detailed model that accounts for the effects of ionic strength as the combined result of one-to-one competition between a toxin molecule and a monovalent cation such as $Na^+$ for a common anionic subsite and electrostatic screening of a negative surface potential due to this subsite and/or other negatively charged groups in the vicinity of the toxin receptor. For a mechanism in which electrostatic interaction is a major determinant of the association rate, one would expect to observe a correlation between $k_a(0)$ and net charge for various toxin derivatives.

In Figure 8 the zero-voltage association rate constants for various toxins are plotted on a logarithmic scale versus the apparent net charge of the toxin for both the m-type channel from normal rate muscle and the h-type channel from canine heart. As described in a preliminary review (Moczydlowski et al., 1986c), we observe a good correlation ($r = 0.97$) between the logarithm of $k_a(0)$ and net charge for the normal rat muscle channel. This behavior follows a Boltzmann relationship with respect to surface potential:

$$k_a = k_a^0 \exp(-z\psi F/RT) \quad (8)$$

where $k_a^0$ is the intrinsic association rate constant at zero surface potential, $z$ is the net charge on the toxin, and $\psi$ is the magnitude of the surface potential at the toxin binding site. Fitting the data for the rat muscle channel in Figure 8 to eq 8, we obtain a value of $1.2 \times 10^6$ $s^{-1}$ $M^{-1}$ for $k_a^0$ and a surface potential of −43 mV at 0.2 M NaCl. Using the Gouy–Chapman theory of surface potential (McLaughlin, 1977), we

Table I: Kinetic Parameters for Blocking of Various Na-Channel Subtypes by Guanidinium Toxins[a]

| | association rate | | dissociation rate | | equilibrium constant | |
|---|---|---|---|---|---|---|
| toxin ($n$)[a] | $k_a(0)$ ($\times 10^6$ $s^{-1}$ $M^{-1}$) | $z_a'$ | $k_d(0)$ ($s^{-1}$) | $z_d'$ | $K_D(0)$ (nM) | $z'$ |
| | | | Rat Brain, n Type | | | |
| TTX (6) | 3.7 ± 0.2 | 0.20 ± 0.03 | 0.073 ± 0.013 | 0.41 ± 0.10 | 20 ± 3 | 0.60 ± 0.14 |
| STX (7) | 27 ± 1 | 0.38 ± 0.04 | 0.071 ± 0.002 | 0.23 ± 0.02 | 2.6 ± 0.1 | 0.61 ± 0.06 |
| NEO (4) | 17 ± 2 | 0.47 ± 0.09 | 0.013 ± 0.001 | 0.28 ± 0.02 | 0.73 ± 0.07 | 0.75 ± 0.14 |
| | | | Rat Muscle, m Type | | | |
| TTX (7) | 4.0 ± 0.2 | 0.19 ± 0.03 | 0.12 ± 0.004 | 0.40 ± 0.02 | 29 ± 1 | 0.60 ± 0.10 |
| STX (6) | 14 ± 0.4 | 0.22 ± 0.02 | 0.064 ± 0.013 | 0.37 ± 0.15 | 4.4 ± 0.9 | 0.59 ± 0.23 |
| B1 (7) | 4.8 ± 0.1 | 0.31 ± 0.02 | 0.86 ± 0.01 | 0.38 ± 0.05 | 180 ± 14 | 0.68 ± 0.09 |
| GTX2 (7) | 6.2 ± 0.3 | 0.26 ± 0.03 | 0.17 ± 0.02 | 0.32 ± 0.06 | 28 ± 3 | 0.58 ± 0.11 |
| C1 (4) | 1.0 ± 0.02 | 0.07 ± 0.01 | 1.7 ± 0.3 | 0.52 ± 0.10 | 1600 ± 300 | 0.59 ± 0.11 |
| GTX3 (7) | 8.9 ± 0.5 | 0.33 ± 0.06 | 0.039 ± 0.004 | 0.29 ± 0.05 | 44 ± 5 | 0.63 ± 0.10 |
| C2 (6) | 0.66 ± 0.05 | 0.32 ± 0.04 | 0.097 ± 0.004 | 0.40 ± 0.02 | 150 ± 10 | 0.72 ± 0.10 |
| NEO (4) | 9.8 ± 1.2 | 0.36 ± 0.10 | 0.012 ± 0.002 | 0.27 ± 0.12 | 1.2 ± 0.2 | 0.63 ± 0.27 |
| B2 (10) | 1.2 ± 0.05 | 0.30 ± 0.03 | 0.23 ± 0.01 | 0.29 ± 0.04 | 190 ± 11 | 0.59 ± 0.08 |
| GTX1 (5) | 2.3 ± 0.1 | 0.20 ± 0.03 | 0.038 ± 0.002 | 0.49 ± 0.03 | 16 ± 1 | 0.69 ± 0.12 |
| C3 (13) | 0.20 ± 0.01 | 0.18 ± 0.01 | 0.42 ± 0.06 | 0.49 ± 0.06 | 2100 ± 300 | 0.68 ± 0.08 |
| dcSTX (9) | 28 ± 0.3 | 0.34 ± 0.03 | 0.29 ± 0.01 | 0.35 ± 0.03 | 10 ± 1 | 0.68 ± 0.06 |
| dcSTX (8)[b] | 32 ± 0.6 | 0.36 ± 0.02 | 0.24 ± 0.01 | 0.44 ± 0.03 | 7.5 ± 0.5 | 0.81 ± 0.06 |
| | | | Denervated Rat Muscle, m Type | | | |
| TTX (5) | 3.1 ± 0.1 | 0.23 ± 0.02 | 0.11 ± 0.01 | 0.44 ± 0.06 | 34 ± 4 | 0.67 ± 0.09 |
| | | | Denervated Rat Muscle, h Type | | | |
| TTX (8) | 0.54 ± 0.02 | 0.28 ± 0.03 | 0.48 ± 0.02 | 0.24 ± 0.02 | 890 ± 35 | 0.52 ± 0.06 |
| STX (12) | 3.5 ± 0.2 | 0.44 ± 0.04 | 0.51 ± 0.02 | 0.21 ± 0.02 | 150 ± 7 | 0.65 ± 0.07 |
| NEO (13) | 2.7 ± 0.1 | 0.38 ± 0.01 | 0.46 ± 0.01 | 0.25 ± 0.01 | 170 ± 4 | 0.63 ± 0.04 |
| | | | Canine Heart, h Type | | | |
| TTX (16) | 0.46 ± 0.04 | 0.19 ± 0.05 | 0.52 ± 0.03 | 0.32 ± 0.03 | 1100 ± 100 | 0.51 ± 0.13 |
| STX (6) | 4.4 ± 0.3 | 0.40 ± 0.04 | 0.45 ± 0.01 | 0.21 ± 0.01 | 100 ± 7 | 0.59 ± 0.06 |
| C1 (11) | 0.44 ± 0.02 | 0.28 ± 0.03 | 1.4 ± 0.1 | 0.42 ± 0.03 | 3100 ± 200 | 0.69 ± 0.07 |
| NEO (17) | 3.2 ± 0.1 | 0.37 ± 0.03 | 0.53 ± 0.03 | 0.23 ± 0.03 | 160 ± 10 | 0.60 ± 0.07 |
| B2 (24) | 0.26 ± 0.02 | 0.44 ± 0.05 | 2.3 ± 0.1 | 0.06 ± 0.03 | 9100 ± 800 | 0.51 ± 0.21 |
| dcSTX (8) | 4.6 ± 0.2 | 0.39 ± 0.03 | 2.0 ± 0.1 | 0.23 ± 0.04 | 430 ± 30 | 0.61 ± 0.10 |

[a] Blocking rate constants measured in the range of −60 to +60 mV were fit to exponential functions of voltage according to eq 5 and 6. $n$ refers to the number of points used in the fit, and the uncertainty of the values refers to the standard deviation derived from the fitting procedure. Parameters for the equilibrium constant were calculated from the ratio of the expressions for the rate constants. [b] In this experiment bilayers were formed from pure phosphatidylserine while in all other experiments neutral lipids were used.

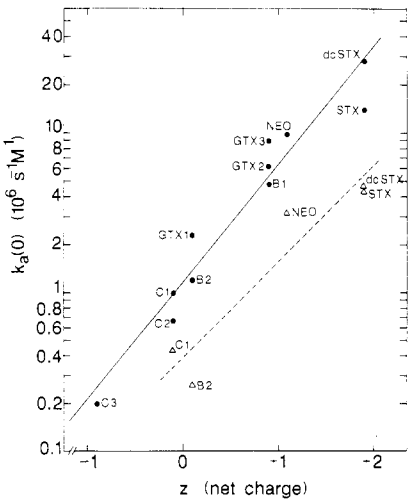


FIGURE 8: Correlation of observed association rate constants for different toxins with net charge of the toxin: (●) data from toxin-sensitive channels of normal rat skeletal muscle; (△) data from toxin-insensitive channels of canine heart. Association rate constants for various toxins were measured at applied voltages from −60 to +60 mV as shown for TTX in Figure 6B. The derived $k_a$ at 0 mV is plotted on a logarithmic scale vs net toxin charge, as calculated from the reported p$K_a$'s of saxitoxin and neosaxitoxin (Rogers & Rapoport, 1980; Shimizu et al., 1978, 1981). Parameters for least-squares fits of the muscle and heart data are given in the text.

obtain a value of 1 $e^-/320$ Å$^2$ as an estimate for the surface charge density.

The results for the canine heart channel in Figure 8 show a similar correlation ($r = 0.95$) between $k_a(0)$ of various STX derivatives and net toxin charge. A fit of the heart data to eq 8 gives values of $k_a^0 = 3.9 \times 10^5$ $s^{-1}$ $M^{-1}$ and $\psi = -35$ mV, at 0.2 M NaCl or 1 $e^-/410$ Å$^2$ for the surface charge density. We may compare our results for m- and h-subtypes with those of Green et al. (1987b) for a canine brain channel that is likely to be an n-type channel (insensitive to μ-conotoxin). The estimated surface charge densities at the toxin receptor are 1/300, 1/320, and 1/410 $e^-/A^2$ for n-, m-, and h-subtypes, respectively, while the estimated $k_a^0$ values for toxins in the absence of surface charge are $3.0 \times 10^6$, $1.2 \times 10^6$, and $0.39 \times 10^6$ $s^{-1}$ $M^{-1}$, respectively. This comparison suggests that the major difference between the TTX-insensitive heart channel and the TTX-sensitive muscle and brain channels is a 3–8-fold lower $k_a^0$ for the heart channel while the surface charge density is relatively constant with only a 30% variation.

To interpret this finding, we must consider that these $k_a^0$ values are about 3 orders of magnitude lower than that expected on the basis of diffusion (Fersht, 1985). The binding rates of many small ligands to enzymes also exhibit values lower than the diffusional collision frequency, and this has often been interpreted by postulating a slow rate-limiting step subsequent to collision (Creighton, 1983). Thus we propose that high- and low-affinity Na-channel subtypes differ in the rate at which the toxin–receptor encounter complex relaxes to a stable bound complex, resulting in different observed values of $k_a^0$.

Our bilayer experiments are normally carried out with membranes formed from neutral lipids in order to minimize the possibility of surface charge effects from lipid head groups. Thus in the preceding discussion, the negative surface potential

is presumed to be mediated by the channel protein. To test whether negatively charged lipids can influence the kinetics of toxin binding, we compared the blocking kinetics of dcSTX, a divalent cationic toxin, in neutral membranes and in membranes formed from pure bovine brain phosphatidylserine. If the toxin binding site is located close to the lipid head groups, we would expect to observe a dramatic increase in the apparent association rate of dcSTX due to the increase in the local concentration of toxin molecules near the membrane. The results of this experiment (Table I) indicate only a 14% increase of the association rate constant and little change in any of the other kinetic parameters. Since the small differences observed between the neutral and negatively charged membranes are close to the error associated with these measurements, we conclude that negative surface charges on lipid head groups have essentially no effect on toxin binding under these conditions.

## Discussion

Collections of related compounds such as those in Figure 7 are useful for evaluating the relative intrinsic binding energy $\Delta G_i$ of chemical substituents as first outlined by Jencks (1981), who proposed that the $\Delta G_i$ of a substituent X can be expressed as

$$\Delta G_i = RT \ln (K_{R-X}/K_R) \quad (9)$$

where $K_{R-X}$ is the equilibrium dissociation constant of a molecule with a certain substituent X and $K_R$ is that of a related molecule where X is absent or replaced by a hydrogen atom. This is considered to be a valid relative measure of intrinsic binding energy when connection of the two parts of the molecule does not lead to differences in loss of entropy or to strain in the bound complex. Recently, this approach was used to measure a value of 4.0 kcal/mol for the intrinsic binding energy of a specific hydrogen bond formed with a ligand amide group in the active site of thermolysin (Bartlett & Marlowe, 1987). In that study five different molecular pairs of inhibitors exhibited the same value of $\Delta G_i$, within 10%, showing that eq 9 is directly applicable to protein–ligand interactions under optimal conditions. However in a case where surface charge effects are evident, eq 9 could give misleading results. For example, a negatively charged substituent might contribute a favorable binding interaction in a binding site, but this favorable binding energy could be offset by a slower association rate if there were a negative surface potential. These effects could cancel leading to no observed difference in equilibrium binding affinity for ligands with and without the substituent. In fact however, the energetics of the binding rates for two molecules with and without the substituent would actually be quite different. Since this situation applies to the present case, it is preferable to compare the relative free energies of activation:

$$\Delta G_a^{\ddagger} = RT \ln (k_{a,R-X}/k_{a,R}) \quad (10)$$

$$\Delta G_d^{\ddagger} = -RT \ln (k_{d,R-X}/k_{d,R}) \quad (11)$$

where eq 10 and 11 refer to the intrinsic binding activation energies for association and dissociation, respectively.

Application of eq 10 to the association reaction can provide an estimate of the energy loss suffered by the addition of three different negatively charged substituents to the saxitoxin molecule. For the m-type Na channel, five pairs of toxin molecules that differ in the substitution of the N-21 sulfo group exhibit a mean $\Delta G_a^{\ddagger}$ of 1.2 ± 0.3 (SD) kcal/mol. Likewise, for six pairs of molecules that differ by a C-11 hydroxysulfate group, the mean $\Delta G_a^{\ddagger}$ is 0.80 ± 0.36 kcal/mol. The N-1 hydroxyl group with its p$K_a$ of 6.75 is incompletely dissociated at pH 7.4, but if we normalize the change in free energy by the charge difference between NEO and STX ($\Delta z = -0.72$), we obtain a mean $\Delta G_a^{\ddagger}$ of 0.88 ± 0.44 kcal/mol for four different molecular pairs differing by this substituent. The addition of one negative charge at any of three positions thus leads to a reduction in the association rate equivalent to about 1 kcal/mol of binding energy. As discussed above this energy loss is probably due to the repulsive interaction of an additional negative charge on the ligand with the negative surface potential in the vicinity of the binding site.

Table II: Effect of Various Substituents on the Dissociation Reaction of Saxitoxin Derivatives[a]

| RX | R | Na-channel subtype | $\Delta G_d^{\ddagger}$ (kcal/mol) |
|---|---|---|---|
| | | X = -OH at N-1 | |
| NEO | STX | m | −0.98 ± 0.20 |
| B2 | B1 | m | −0.77 ± 0.20 |
| GTX1 | GTX2 | m | −0.88 ± 0.10 |
| C3 | C1 | m | −0.82 ± 0.14 |
| NEO | STX | n | −0.99 ± 0.08 |
| NEO | STX | h[b] | 0.10 ± 0.01 |
| NEO | STX | h[c] | −0.06 ± 0.01 |
| | | X = $-CONH_2$ at O-14 | |
| STX | dcSTX | m | −0.89 ± 0.18 |
| STX | dcSTX | h[b] | −0.87 ± 0.04 |
| | | X = $-SO_3^-$ at N-21 | |
| B1 | STX | m | 1.5 ± 0.3 |
| C1 | GTX2 | m | 1.4 ± 0.2 |
| C2 | GTX3 | m | 0.53 ± 0.05 |
| B2 | NEO | m | 1.7 ± 0.3 |
| C3 | GTX1 | m | 1.4 ± 0.2 |
| B2 | NEO | h[b] | 0.86 ± 0.05 |

[a] The chemical substituents R and RX refer to the structures of saxitoxin derivatives listed in Figure 7. The relative free energy contributed to the reaction by these substituents was calculated for various Na-channel subtypes according to eq 11 with the data of Table I. [b] Toxin-insensitive subtype from canine heart. [c] Toxin-insensitive subtype from denervated muscle.

Application of eq 11 can be used to evaluate the contribution of various substituents to the energy required to dissociate the ligand–receptor complex. This approach shows that the N-1 hydroxyl group provides a favorable binding interaction for the high-affinity m and n subtypes but not for the h subtype. The m-type channel exhibits a mean $\Delta G_d^{\ddagger}$ of −0.86 ± 0.09 kcal/mol for four different molecular pairs, and the n-type channel exhibits a similar value of −0.99 kcal/mol for the NEO/STX pair (Table II). The low-affinity subtypes from heart and denervated muscle both show essentially no difference in the dissociation rates of NEO and STX, or $\Delta G_d^{\ddagger}$ values of less than 0.1 kcal/mol. This result implies that a chemical interaction with this substituent is missing in the h-type Na channel. The N-1 hydroxyl group with its low p$K_a$ of 6.75 (Shimizu et al., 1978) could serve either as a H-bond donor in the protonated form or a H-bond acceptor in either the protonated or deprotonated forms. Previous equilibrium studies have shown that NEO has a higher affinity than STX at low pH and a lower affinity than STX at high pH (Strichartz, 1984; Kao et al., 1983; Kao, 1986). This suggests that the protonated hydroxyl provides a stabilizing interaction and favors the role of the hydroxyl group as an H-bond donor.

The carbamoyl side chain also contributes favorably to the binding affinity of STX as previously suggested by the equilibrium studies of Kao and Walker (1982). A comparison of the dissociation rates of dcSTX and STX shows that this substituent exhibits a $\Delta G_d^{\ddagger}$ of −0.89 kcal/mol for the m-type channel and −0.87 kcal/mol for the h-type channel from heart (Table II). Similar to the case of the N-1 hydroxyl group,

this binding energy could be due to a specific hydrogen bond since the carbamoyl tail contains both amide and carbonyl groups. However, this putative hydrogen bond appears to be conserved in both high- and low-affinity subtypes.

Similar calculations show that the N-21 sulfo group destabilizes the toxin–receptor complex with a mean $\Delta G_d^{\ddagger}$ of 1.3 ± 0.4 kcal/mol for the m-type channel (five different molecular pairs, Table II). The addition of this substituent appears to perturb the favorable interaction with the carbamate group. If the terminal amide serves as a hydrogen-bond donor, the sulfo group may disrupt this bond. This effect is also observed in the B2/NEO toxin pair for the heart channel, again suggesting conserved chemical interactions in this region of the binding site.

Our work demonstrates that the insensitivity of h-type Na channels to TTX and STX survives transfer to an artificial bilayer and suggests that this pharmacological characteristic is a not readily reversible consequence of membrane environment. This is in contrast to the case of $\alpha$-scorpion toxin binding to rat brain Na channels, where it was found that high-affinity binding to reconstituted channels is dependent upon the presence of phosphatidylethanolamine and phosphatidylserine in the membrane (Feller et al., 1985). In light of the isolation of multiple Na-channel cDNA clones from rat brain (Noda et al., 1986), it is likely that the subtype differences encountered here are the manifestation of distinct but homologous primary structures. A similar situation occurs in the case of the catalytic subunit of ($Na^+$,$K^+$)-ATPase, where an ouabain-insensitive enzyme from rat brain and an ouabain-sensitive enzyme from rat kidney differ in primary sequence (Shull et al., 1986). Considering the evidence for multiple types of other membrane channels such as Ca channels (Nowycky et al., 1985) and nicotinic acetylcholine receptor channels (Conti-Tronconi et al., 1985), a multiplicity of subtypes may be a widespread feature of membrane transport proteins in vertebrates.

The presence of negatively charged groups on the extracellular surface of Na channels is supported by a considerable body of evidence including effects of inorganic cations and pH on toxin binding (Henderson et al., 1974; Hille et al., 1975; Reed & Raftery, 1976; Barchi & Weigele, 1979; Grissmer, 1984), gating kinetics (Frankenhaeuser & Hodgkin, 1957; Campbell & Hille, 1976), and conduction (Woodhull, 1973; Green et al., 1987b) and the effect of chemical modification of carboxyl groups on these functional properties (Spalding, 1980; Sigworth & Spalding, 1980; Worley et al., 1986). From a structural viewpoint negative charges could exert their influence over these functions from three main locations: glutamate and aspartate groups on the channel protein in an exposed polar environment, acidic phospholipids surrounding the channel, and sialic acid residues (Miller et al., 1983) on the carbohydrate portion of the major glycoprotein that forms the channel.

Green et al. (1987a,b) have recently estimated the external surface charge density that is sensed by TTX/STX binding (1 $e^-$/300 Å$^2$) and $Na^+$ conduction (1 $e^-$/260 Å$^2$) using batrachotoxin-activated Na channels from canine brain in neutral bilayers. In agreement with our results, they also found that negatively charged phospholipids do not increase the apparent surface charge over that sensed by these processes in neutral lipids. This implies that the toxin binding site and channel mouth are located far (>20 Å) from lipid head groups, which is quite possible for a 208 000-dalton protein (Numa & Noda, 1986) expected to have an approximate radius of 39 Å on the basis of a sphere of protein with this mass. After ruling out a contribution from lipid, lack of structural information prevents evaluation of the relative contribution of protein and sugar residues to observed surface charge effects. The chemical analysis of Miller et al. (1983) provides an estimate of about 100 sialic acid groups per Na-channel glycopeptide. If this amount of charge were confined to a plane with the expected area of the extracellular surface of a protein as large as the Na channel, the density of negative charge would exceed our measured value of surface charge density by about 6-fold. It is therefore conceivable that the negatively charged carbohydrate could hang like a cloud over the channel and serve to locally concentrate inorganic cations and cationic toxins. However, if cation channels do indeed use negative charge for this purpose, acidic residues located at functional sites on the protein surface would be more effective in directing ions to these sites. Future studies of deglycosylated channels will be required to resolve this issue.

In addition to our work, previous functional comparisons of different Na-channel subtypes suggest that subtype differences are not due to major differences in surface charge. Campbell and Hille (1976) found the same electrostatic effects in a comparison of gating for nerve and muscle Na channels, and Huang et al. (1979) found that ion selectivity and the effect of pH on $Na^+$ permeability and TTX inhibition are the same for a TTX-sensitive and a TTX-insensitive neuroblastoma cell line. In our view the lower association rate constant for toxin binding to h-type channels arises from a slower conformational relaxation of the protein before or after collision of the toxin with the site. The possibility that Na-channel subtypes might differ with respect to other conformational properties such as gating kinetics deserves careful comparison studies. Along these lines, Campbell and Hille (1976) found that the gating activation process of Na channels is about 5 times faster in frog nerve than muscle when measured under the same conditions.

With data from equilibrium studies of the relative potency of TTX, STX, and derivatives of these toxins, previous workers have proposed detailed models of the chemical interactions between functional groups of these toxins and the receptor site (Hille, 1975; Strichartz, 1984; Kao, 1986). In the present study we have obtained additional evidence of hydrogen bonds with the N-1 hydroxyl group in NEO (for n and m subtypes) and the carbamate side chain (for m and h subtypes). Our data suggest that the intrinsic binding energy associated with these latter two putative hydrogen bonds is on the order of a factor of 5 in rate enhancement or about 1 kcal/mol. Quite similar values of 0.5–1.2 kcal/mol have been reported for hydrogen bonds with various uncharged ligand hydroxyl groups in the active site of tyrosyl-tRNA-synthetase (Fersht et al., 1985). While we have observed a missing interaction with the N-1 hydroxyl group of NEO in h-type Na channels, we have not yet identified the lost bonds responsible for the faster dissociation of TTX and STX from the h-subtype Na-channel receptor. The 4–8-fold difference in dissociation rate of these toxins between high- and low-affinity subtypes is small enough to be accounted for by only one hydrogen bond. Possible candidates would be a missing hydrogen bond to one of the cis C-12 hydroxyl groups in STX or to either the C-9 or C-10 hydroxyl groups of TTX, which have been suggested to bind in homologous orientations (Kao & Walker, 1982). Future bilayer studies with the appropriate toxin derivatives may permit these critical groups to be identified.

ACKNOWLEDGMENTS

We are grateful to Dr. John W. Daly of the Laboratory of Bioorganic Chemistry at NIH for the gift of batrachotoxin.

## REFERENCES


Baer, M., Best, P. M., & Reuter, H. (1976) *Nature (London) 263*, 344–345.

Barchi, R. L. (1986) *Ann. N.Y. Acad. Sci. 479*, 179–185.

Barchi, R. L., & Weigele, J. B. (1979) *J. Physiol. (London) 295*, 383–396.

Bartlett, P. A., & Marlowe, C. K. (1987) *Science (Washington, D.C.) 235*, 569–571.

Brown, A. M., Lee, K. S., & Powell, T. (1981) *J. Physiol. (London) 318*, 479–500.

Campbell, D. T., & Hille, B. (1976) *J. Gen. Physiol. 67*, 309–323.

Catterall, W. A. (1984) *Science (Washington, D.C.) 223*, 653–661.

Catterall, W. A., & Coppersmith, J. (1981) *Mol. Pharmacol. 20*, 526–532.

Cohen, C. J., Bean, B. P., Colatsky, T. J., & Tsien, R. W. (1981) *J. Gen. Physiol. 78*, 383–411.

Colquhoun, D., & Hawkes, A. G. (1983) in *Single-Channel Recording* (Sakmann, B., & Neher, E., Eds.) pp 135–175, Plenum, NY.

Conti-Tronconi, B. M., Dunn, S. M. J., Barnard, E. A., Dolly, J. O., Lai, F. A., Ray, N., & Raftery, M. A. (1985) *Proc. Natl. Acad. Sci. U.S.A. 82*, 5208–5212.

Creighton, T. E. (1983) *Proteins: Structures and Molecular Principles*, Freeman, New York.

Cruz, L. J., Gray, W. R., Olivera, B. M., Zeikus, R. D., Kerr, L., Yoshikami, D., & Moczydlowski, E. (1985) *J. Biol. Chem. 260*, 9280–9288.

DeCoursey, T. E., Bryant, S. H., & Owenburg, K. M. (1981) *Am. J. Physiol. 240*, C56–C63.

Feller, D. J., Talvenheimo, J. A., & Catterall, W. A. (1985) *J. Biol. Chem. 260*, 11542–11547.

Fersht, A. (1985) *Enzyme Structure and Mechanism*, Freeman, New York.

Fersht, A. R., Shi, J. P., Knill-Jones, J., Lowe, D. M., Wilkinson, A. J., Blow, D. M., Brick, P., Carter, P., Waye, M. M. Y., & Winter, G. (1985) *Nature (London) 314*, 235–238.

Frankenhaueser, B., & Hodgkin, A. L. (1957) *J. Physiol. (London) 137*, 218–244.

Frelin, C., Vijverberg, H. P. M., Romey, G., Vigne, P., & Lazdunski, M. (1984) *Pfluegers Arch. 402*, 121–128.

Frelin, C., Cognard, C., Vigne, P., & Lazdunski, M. (1986) *Eur. J. Pharmacol. 122*, 245–250.

French, R. J., Worley, J. F., III, & Krueger, B. K. (1984) *Biophys. J. 45*, 301–310.

Fritz, L. C., Moore, H. P. H., Raftery, M. A., & Brockes, J. P. (1983) *Cold Spring Harbor Symp. Quant. Biol. 48*, 181–185.

Ghazarossian, V. E., Schantz, E. J., Schnoes, H. K., & Strong, F. M. (1976) *Biochem. Biophys. Res. Commun. 68*, 776–780.

Gonoi, T., Sherman, S. J., & Catterall, W. A. (1985) *J. Neurosci. 5*, 2559–2564.

Green, W. N., Weiss, L. B., & Anderson, O. S. (1987a) *J. Gen. Physiol. 89*, 841–872.

Green, W. N., Weiss, L. B., & Anderson, O. S. (1987b) *J. Gen. Physiol. 89*, 873–903.

Grissmer, S. (1984) *Pfluegers Arch. 402*, 353–359.

Guo, X., Bryant, S. H., & Moczydlowski, E. G. (1986) *Biophys. J. 49*, 380a.

Hall, S. (1982) Ph.D. Thesis, University of Alaska, Fairbanks, AK.

Hartshorne, R. P., & Catterall, W. A. (1984) *J. Biol. Chem. 259*, 1667–1675.

Hartshorne, R. P., Keller, B. U., Talvenheimo, J. A., Catterall, W. A., & Montal, M. (1985) *Proc. Natl. Acad. Sci. U.S.A. 82*, 240–244.

Henderson, R., Ritchie, J. M., & Strichartz, G. R. (1974) *Proc. Natl. Acad. Sci. U.S.A. 71*, 3936–3940.

Hille, B. (1975) *Biophys. J. 15*, 615–619.

Hille, B., Ritchie, J. M., & Strichartz, G. R. (1975) *J. Physiol. (London) 250*, 34P–35P.

Huang, L. M., Catterall, W. A., & Ehrenstein, G. (1979) *J. Gen. Physiol. 73*, 839–854.

Jencks, W. P. (1981) *Proc. Natl. Acad. Sci. U.S.A. 78*, 4046–4050.

Kao, C. Y. (1986) *Ann. N.Y. Acad. Sci. 479*, 52–67.

Kao, C. Y., & Walker, S. E. (1982) *J. Physiol. (London) 323*, 619–637.

Kao, P. N., James-Kracke, M. R., & Kao, C. Y. (1983) *Pfluegers Arch. 398*, 199–203.

Khodorov, B. I. (1985) *Prog. Biophys. Mol. Biol. 45*, 57–148.

Kraner, S. D., Tanaka, J. C., & Barchi, R. L. (1985) *J. Biol. Chem. 260*, 6341–6347.

Krueger, B. K., Worley, J. F., III, & French, R. J. (1983) *Nature (London) 303*, 172–175.

Krueger, B. K., Worley, J. F., III, & French, R. J. (1986) *Ann. N.Y. Acad. Sci. 479*, 257–268.

McLaughlin, S. (1977) *Curr. Top. Membr. Transp. 9*, 71–144.

Miller, J. A., Agnew, W. S., & Levinson, S. R. (1983) *Biochemistry 22*, 462–470.

Moczydlowski, E. G., & Latorre, R. (1983) *Biochim. Biophys. Acta 732*, 412–420.

Moczydlowski, E., Garber, S. S., & Miller, C. (1984a) *J. Gen. Physiol. 84*, 665–686.

Moczydlowski, E., Hall, S., Garber, S. S., Strichartz, G. R., & Miller, C. (1984b) *J. Gen. Physiol. 84*, 687–704.

Moczydlowski, E., Olivera, B. M., Gray, W. R., & Strichartz, G. R. (1986a) *Proc. Natl. Acad. Sci. U.S.A. 83*, 5321–5325.

Moczydlowski, E., Uehara, A., Guo, X., & Heiny, J. (1986b) *Ann. N.Y. Acad. Sci. U.S.A. 479*, 269–292.

Moczydlowski, E., Uehara, A., & Hall, S. (1986c) in *Ion Channel Reconstitution* (Miller, C., Ed.) pp 405–428, Plenum, New York.

Mueller, P., & Rudin, D. O. (1969) *Curr. Top. Membr. Transp. 3*, 157–249.

Noda, M., Ikeda, T., Kayano, T., Suzuki, H., Takeshima, H., Kurasaki, M., Takahashi, H., & Numa, S. (1986) *Nature (London) 320*, 188–192.

Nowycky, M. C., Fox, A. P., & Tsien, R. W. (1985) *Nature (London) 316*, 440–443.

Numa, S., & Noda, M. (1986) *Ann. N.Y. Acad. Sci. 479*, 338–355.

Ohizumi, Y., Nakamura, H., Kobayashi, J., & Catterall, W. A. (1986) *J. Biol. Chem. 261*, 6149–6152.

Pappone, P. A. (1980) *J. Physiol. (London) 306*, 377–410.

Redfern, P., & Thesleff, S. (1971) *Acta Physiol. Scand. 82*, 70–78.

Reed, J. K., & Raftery, M. A. (1976) *Biochemistry 15*, 944–953.

Ritchie, J. M. & Rogart, R. B. (1977) *Rev. Physiol., Biochem. Pharmacol. 79*, 1–50.

Rogart, R. B. (1986) *Ann. N.Y. Acad. Sci. 479*, 402-430.
Rogers, R. S., & Rapoport, H. (1980) *J. Am. Chem. Soc. 102*, 7335-7339.
Rosemblatt, M., Hidalgo, C., Vergara, C., & Ikemoto, N. (1981) *J. Biol. Chem. 256*, 8140-8148.
Shimizu, Y., Hsu, C., Fallon, W. E., Oshima, Y., Miura, I., & Nokanishi, K. (1978) *J. Am. Chem. Soc. 100*, 6791-6793.
Shimizu, Y., Hsu, C., & Genenah, A. (1981) *J. Am. Chem. Soc. 103*, 605-609.
Shull, G. E., Greeb, J., & Lingrel, J. B. (1986) *Biochemistry 25*, 8125-8132.
Sigworth, F. J. (1983) in *Single Channel Recording* (Sakmann, B., & Neher, E., Eds.) pp 3-35, Plenum, New York.
Sigworth, F. J., & Spalding, B. C. (1980) *Nature (London) 283*, 293-295.
Spalding, B. C. (1980) *J. Physiol. (London) 305*, 485-500.
Strichartz, G. (1984) *J. Gen. Physiol. 84*, 281-305.
Strichartz, G., Rando, T., Hall, S., Gitschier, J., Hall, L., Magnani, B., & Hansen-Bay, C. (1986) *Ann. N.Y. Acad. Sci. 479*, 96-112.
Van Alstyne, E., Burch, R. M., Knickelbein, R. G., Hungerford, R. T., Gower, E. J., Webb, J. G., Poe, S. L., & Lindenmayer, G. E. (1980) *Biochim. Biophys. Acta 602*, 131-143.
Weiss, R. E., & Horn, R. (1986) *Science (Washington, D.C.) 233*, 361-364.
Wollner, D. A., & Catterall, W. A. (1985) *Brain Res. 331*, 145-149.
Woodhull, A. M. (1973) *J. Gen. Physiol. 61*, 687-708.
Worley, J. F., III, French, R. J., & Krueger, B. K. (1986) *J. Gen. Physiol. 87*, 327-349.

# Desensitization of γ-Aminobutyric Acid Receptor from Rat Brain: Two Distinguishable Receptors on the Same Membrane†

Derek J. Cash* and Katragadda Subbarao‡

*Neurochemistry Unit, Missouri Institute of Psychiatry, and Department of Biochemistry, School of Medicine, University of Missouri—Columbia, St. Louis, Missouri 63139*

*Received May 12, 1987; Revised Manuscript Received August 11, 1987*

ABSTRACT: Transmembrane chloride flux mediated by γ-aminobutyric acid (GABA) receptor can be measured with a mammalian brain homogenate preparation containing sealed membrane vesicles. The preparation can be mixed rapidly with solutions of defined composition. Influx of $^{36}Cl^-$ tracer initiated by mixing with GABA was rapidly terminated by mixing with bicuculline methiodide. The decrease in the isotope influx measurement due to prior incubation of the vesicle preparation with GABA, which increased with preincubation time and GABA concentration, was attributed to desensitization of the GABA receptor. By varying the time of preincubation with GABA between 10 ms and 50 s with quench-flow technique, the desensitization rates could be measured over their whole time course independently of the chloride ion flux rate. Most of the receptor activity decreased in a fast phase of desensitization complete in 200 ms ($t_{1/2}$ = 32 ms) at saturation with GABA. Remaining activity was desensitized in a few seconds ($t_{1/2}$ = 533 ms). These two phases of desensitization were each kinetically first order and were shown to correspond with two distinguishable GABA receptors on the same membrane. The receptor activities could be estimated, and the faster desensitizing receptor was the predominant one, giving on average ca. 80% of the total activity. The half-response concentrations were similar, 150 and 114 μM for the major and minor receptors, respectively. The dependence on GABA concentration indicated that desensitization is mediated by two GABA binding sites. The fast desensitization rate was approximately 20-fold faster than previously reported rates while the slower desensitization rate was slightly faster than previously reported rates.

The γ-aminobutyric acid (GABA) receptor is the major inhibitory neurotransmitter receptor in the mammalian brain. It is crucial in controlling the excitability of neurones (Enna & Gallagher, 1983; Krnjevic, 1974). Electrophysiological experiments showed that a GABA-induced increase in transmembrane potential at postsynaptic membrane is caused by an increase in its permeability to chloride ion. Measurements with radioactive chloride have supported this, with brain slices (Wong et al., 1984) and cultured neurones (Thampy & Barnes, 1984). Subsequently, GABA-mediated transmembrane chloride flux was demonstrated with membrane preparations containing vesicles from brain homogenate of rat or mouse (Allan et al., 1985; Subbarao & Cash, 1985; Sânchez et al., 1984; Schwartz et al., 1986a). The pharmacology of this response corresponded with the $GABA_A$-type receptor (Harris & Allan, 1985). This type of preparation can be mixed rapidly with solutions of known composition, allowing biochemical studies of the responses of the GABA receptor to be made.

A number of channel-forming neurotransmitter receptors are desensitized by their neurotransmitter. During exposure to the neurotransmitter, in times much longer than the channel-opening reaction, the receptor is transformed to a state that does not form open channels. Desensitization of GABA receptor has been observed with electrophysiological techniques (Krnjevic, 1981) in hippocampal neurones (Ozawa & Yuzaki, 1984; Numann & Wong, 1984; Thalman & Hershkowitz, 1985), in ganglion cells (Gallagher et al., 1983; Adams & Brown, 1975; Hackman et al., 1982; Akaiki et al., 1985), in rat brain receptor expressed in oocytes (Houamed et al., 1984;

† This work was supported in part by a grant from the Research Council of the University of Missouri—Columbia Medical School.
‡ Recipient of a Missouri Institute of Psychiatry fellowship.

0006-2960/87/0426-7556$01.50/0 